OPEN ACCESS

ARTICLE

Journal homepage: www.the-innovation.org/energy-use

Energy Use

INNOVATION PRESS

Energy Use 1 (2025):100003

Contents lists available at INNOVATION PRESS

# Coordinated Optimization of Carbon-Electricity-Gas Trading in Multi-Vector Energy Systems across Buildings

**Dafeng Zhu,[1] Ivan Korolija,[1] Zhao Yang Dong,[2] Dejan Mumovic,[1] Seungjae Lee,[3] and Rui Tang[1,*]**

*Correspondence: rui.tang@ucl.ac.uk

Received: August 21, 2025; Accepted: September 24, 2025; Published Online: September 25, 2025; https://doi.org/10.59717/ipj.energy-use.2025.100003



## GRAPHICAL ABSTRACT


## PUBLIC SUMMARY

- Evolution of thermodynamic cycles enhancing energy storage density, efficiency, and adaptability.
- Uses enhanced Lyapunov optimization for real-time stochastic decision-making.
- Introduces dynamic storage pricing and auction-based energy trading.
- Case studies show improved energy efficiency, battery use, and cost savings.
- Achieves near-optimal cost with combined emission reduction and efficiency.

ARTICLE

OPEN ACCESS

Journal homepage: www.the-innovation.org/energy-use

Energy Use

INNOVATION PRESS

Energy Use 1 (2025):100003

Contents lists available at INNOVATION PRESS

# Coordinated Optimization of Carbon-Electricity-Gas Trading in Multi-Vector Energy Systems across Buildings

**Dafeng Zhu,[1] Ivan Korolija,[1] Zhao Yang Dong,[2] Dejan Mumovic,[1] Seungjae Lee,[3] and Rui Tang[1,*]**

[1]Institute for Environmental Design and Engineering, University College London, London WC1E 6BT, UK

[2]Department of Electrical Engineering, City University of Hong Kong, Hong Kong SAR, China

[3]Department of Civil and Mineral Engineering, University of Toronto, Toronto M5S 1A4, Canada

*Correspondence: rui.tang@ucl.ac.uk

Received: August 21, 2025; Accepted: September 24, 2025; Published Online: September 25, 2025; https://doi.org/10.59717/ipj.energy-use.2025.100003



Citation: Zhu D., Korolija I., Dong Z. Y., et al. (2025). Coordinated Optimization of Carbon-Electricity-Gas Trading in Multi-Vector Energy Systems across Buildings. *Energy Use* 1:100003.

High building power demand contributes significantly to carbon emissions and places considerable stress on power grid energy supply. While control and optimization methods in buildings can effectively reduce energy consumption and reshape load profiles, existing approaches often overlook the strong coupling between energy and carbon, and lack real-time, incentive-compatible mechanisms to coordinate operations across buildings and distributed energy resources. To address these limitations, this study develops a synergistic carbon–electricity–gas trading mechanism to optimize the operation of multiple buildings integrated with multi-vector energy systems, targeting improved energy efficiency, cost reduction, and emission mitigation. An enhanced Lyapunov optimization approach is proposed to transform the long-term stochastic optimization problem into a series of online-solvable subproblems, maximizing the benefits of energy storage systems and enabling efficient real-time decision-making at each operational time slot. Additionally, a dynamic storage-based pricing mechanism is introduced to reflect true trading demands, complemented by an auction-based matching strategy to facilitate inter-building energy trading. Case studies conducted on five UK campus buildings demonstrate that the proposed mechanism enhances energy efficiency and battery performance, and asymptotically approaches optimal cost performance through calibrated weighting and auxiliary parameters.

## INTRODUCTION

Buildings, as the primary environment for human habitation and activity, are the main contributor to global energy consumption and carbon emissions, accounting for over 34 % of global energy use and carbon emissions in 2023.[1] With continued urbanization and growing global population, building-related energy use and emissions are expected to increase further. To alleviate these challenges in buildings, it is essential to optimize and coordinate multiple types of energy source and storage loads,[2] such as electricity, natural gas; batteries, thermal energy storage (TES) tanks; heating, ventilation and air conditioning (HVAC), and lighting.

Distributed energy resources (DERs), such as photovoltaic (PV) systems and batteries, can enhance building energy efficiency and reduce carbon emissions. They achieve this by minimizing transmission losses, displacing fossil fuel usage, flattening peak demand, and providing reliable backup energy supply.[3] Notably, batteries serve as a key enabler for addressing supply-demand imbalances through cost-effective peak shaving and load management. Their adoption in buildings is experiencing consistent growth, driven by declining technology costs. Many studies have investigated distributed energy resources, especially storage systems, in buildings.[4] Plytaria et al.[5] constructed an energy scheduling and management model for a building microgrid with battery and PV systems to improve the operational performance of the flexible resource in the building. Nikkhah et al.[6] presented a multi-level energy management mechanism in the residential building controller to utilize the flexibility provided by storage to reshape the building load and secure occupant comfort. He et al.[7] deployed model predictive control to coordinate various distributed renewable energy and appliances to achieve energy balance. Saberi et al.[8] adopted a multi-agent deep Q-learning mechanism to adjust flexible appliances and deal with the uncertainties of PV generation in real-time. Although building energy management supports the integration of distributed energy resources and aids in balancing power grids, inherent supply-demand mismatches necessitate coordinated operation among individual buildings.

To further enhance energy efficiency and balance at scales, energy market liberalization reforms are being accelerated, supported by coordinated energy storage deployment.[9] Meanwhile, advances in communication and smart grid technologies have enabled energy sharing and distributed coordination among buildings, effectively improving energy utilization and overall efficiency. Jin et al.[10] presented a peer-to-peer energy trading mechanism among buildings and considered their thermal dynamics to improve economic benefits and explore the heating load flexibility. Zheng et al.[2] adopted a distributed coordination method to coordinate thermal loads of buildings, which optimized the energy flexibility utilization in a scalable manner. Yu et al.[11] designed a distributed operation method based on regularized policy iteration to coordinate buildings' operations and minimize the total peak demand violation of all buildings. Yang et al.[12] constructed an energy sharing model for multibuildings based on coalition game considering energy storage sizing and cost, which achieved energy arbitrage and benefit enhancement. While existing studies have advanced building energy management through coordinated scheduling and energy sharing strategies-improving load flexibility and operational efficiency few studies consider carbon emission mitigation and the synergistic integration of multi-technology decarbonization approaches.

Since 2015, carbon emissions reduction from buildings have fallen far short of the 28% reduction target by 2030 set by the Paris Agreement. To achieve climate resilience and net-zero carbon targets of buildings, a combination of diverse carbon reduction strategies is necessary. For the perspective of demand-side, the emissions of buildings are calculated as the product of energy consumption and the corresponding carbon intensity factor.[13] Once emissions are accurately quantified and their sources identified, reduction efforts can be pur- sued through various paradigms, several of which have been extensively studied. Yang et al.[14] integrated multiple carbon reduction approaches into the build- ing integrated energy system including power-to-grid (P2G), combined heat and power (CHP) and gas boiler to enable low-carbon operations. Yan et al.[15] constructed a two-level carbon trading framework with optimal carbon prices customization and competitive auction model to incentive low-carbon energy consumption. Yu et al.[16] proposed a combined data-driven and model-based optimization mechanism for hydrogen-based building systems to reduce opera- tion costs and emissions. While existing studies have advanced carbon mitigation in building energy systems (BESs), few studies address the co-optimization of carbon-energy markets for synergistic efficiency improvement and emission reduction. The carbon emission nature of energy generation creates tight coupling between energy scheduling and carbon footprints. These challenges are compounded by demand uncertainties and renewable variability, posing significant barriers to building energy conservation and decarbonization.

Targeting at building energy systems, an optimization mechanism that deals with carbon-energy coupling and supply-demand uncertainties is essential. Unlike traditional optimization methods,[17] Lyapunov optimization provides a lightweight online computational alternative that operates without requiring forecasting or historical datasets. Yu et al.[18] proposed a Lyapunov optimization-based method to online control indoor temperature and optimize the costs in commercial buildings. Shi et al.[19] presented a two timescale optimization method for battery storage system (BSS) based on Lyapunov optimization to relax the temporal coupling and relieve the calculation complexity. But existing Lyapunov optimization-based methods are less applied to ensure optimal BSS charging/discharging while accounting for degradation costs.

To address the above challenges, this paper proposed a low-complexity optimization framework based on Lyapunov optimization to facilitate carbon–energy trading among buildings. A storage-based pricing scheme was first developed to determine preliminary trading prices for BESs. Then, enhanced Lyapunov optimization was applied to derive the optimal energy quantities for market submission. A clearing mechanism subsequently finalized the energy transaction volumes and clearing prices, leveraging the synergies of carbon capture (CC) and carbon trading to reduce emissions. Finally, overall system performance was optimized through drift-plus-penalty minimization. The main contributions of this paper are summarized as below:

1. A novel carbon-aware integrated energy optimization framework is proposed, integrating multi-energy storage, CHP units, CC and P2G devices. The synergistic operation of multi-energy storage, CC and P2G devices maximizes renewable energy utilization, enables low-carbon system operation, and enhances overall efficiency by converting captured carbon emissions into synthetic gas, enabling resources circular utilization.

2. To address energy supply-demand mismatches and carbon emission/quota discrepancies among BESs, an integrated electricity-gas trading model coupled with a tiered incentive-penalty mechanism for carbon trading and CC is developed, where emissions are calculated based on carbon emission intensities of multi-energy flows. In addition, an energy storage-based pricing mechanism is presented to guarantee the economic benefits of BESs.

3. To enable real-time carbon-energy trading and scheduling, an enhanced Lyapunov optimization approach is designed to transform the optimiza- tion problem into solvable per-time-slot subproblems, where an auxiliary variable is incorporated to ensure net benefits from BSS charging and discharging under degradation constraints. Finally, an auction-based clearing mechanism is presented to resolve trading problems among BESs.

The remainder of this paper is as follows. The multi-energy device modeling, the integrated energy-carbon trading framework among BESs and optimization objective are presented in Section: system model. Section of solution mechanism details enhanced Lyapunov optimization, pricing and clearing mechanism, and its theoretical performance analysis. Numerical case studies and simulation results are examined in Section: simulation cases. Conslusion summarizes key findings and identifies promising directions for subsequent investigations.

## MATERIALS AND METHODS

### System model

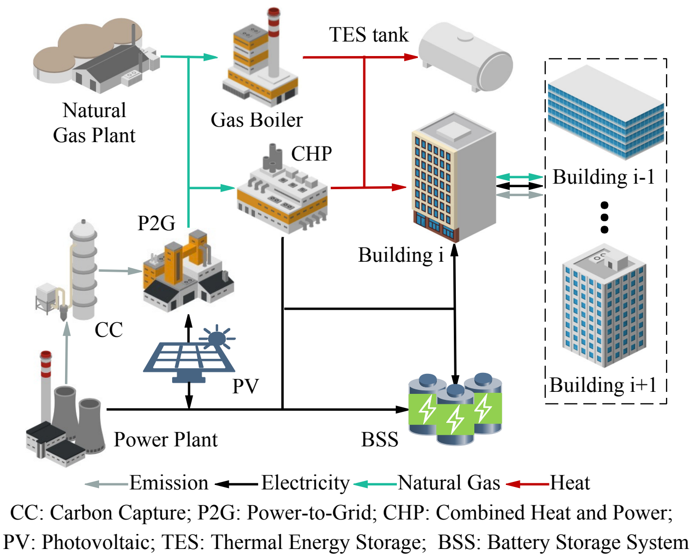


**Figure 1. Low-carbon multi-energy management among BESs**

Figure 1 illustrates a low-carbon multi-energy management system comprising $N$ BESs, a carbon capture power plant (CCPP) and a gas plant, operating over

discrete time slots $t \in \Gamma = \{0, 1, \ldots\}$. For each BES i (where $\forall i \in \{1, 2, \cdots, N\}$, and $N$ is the total number of BESs), associated BSS and other energy devices are referred to as BSS i and devices i, respectively. The CCPP integrates a carbon capture unit with a conventional power plant, allowing dynamic adjustment of carbon capture levels by modulating the capture device's power output—thereby optimizing carbon reduction costs.

### Multi–energy devices

The BSS and TES tank dynamic models of BES i are

$$E^{BSS}_{i,t+1} = E^{BSS}_{i,t} + E^{C}_{i,t} - E^{D}_{i,t}, \quad \forall i,t \tag{1}$$

$$H^{TES}_{i,t+1} = H^{TES}_{i,t} + H^{C}_{i,t} - H^{D}_{i,t}, \quad \forall i,t \tag{2}$$

$$0 \le E^{BSS}_{i,t} \le \overline{E}^{BSS}_{i}, \quad 0 \le H^{TES}_{i,t} \le \overline{H}^{TES}_{i}, \quad \forall i,t \tag{3}$$

$$0 \le E^{C}_{i,t} \le b^{E}_{i,t}\overline{E}^{C}_{i}, \quad 0 \le E^{D}_{i,t} \le (1-b^{E}_{i,t})\overline{E}^{D}_{i}, \quad \forall i,t \tag{4}$$

$$0 \le H^{C}_{i,t} \le \overline{H}^{C}_{i}, \quad 0 \le H^{D}_{i,t} \le \overline{H}^{D}_{i}, \quad \forall i,t \tag{5}$$

*where* $E^{BSS}_{i,t}$, $E^{C}_{i,t} = \eta^{CB}_i P^{CB}_{i,t} \triangle t$ *and* $E^{D}_{i,t} = \frac{1}{\eta^{DB}_i} P^{DB}_{i,t} \triangle t$ are the stored electricity, charging energy, and discharging energy of BSS i at time t, respectively. *where* $E^{TES}_{i,t}$, $H^{C}_{i,t} = \eta^{CT}_i Q^{CT}_{i,t} \triangle t$ *and* $H^{D}_{i,t} = \frac{1}{\eta^{DT}_i} Q^{DT}_{i,t} \triangle t$ denote the stored thermal energy, thermal energy input, and thermal energy output of TES tank i. $\triangle t$ is the length of each time slot. The binary variable *where* $b^{E}_{i,t}$ enforces the constraint that charging and discharging operations cannot occur simultaneously for BSS i at time t. η and P denote the effciency and output power, respectively.

The gas boiler and P2G device models of BES i are as follows

$$H^{B}_{i,t} = \eta^{BG}_i G^{B}_{i,t}, \quad 0 \le H^{B}_{i,t} \le \overline{H}^{B}_{i} \tag{6}$$

$$G^{P2G}_{i,t} = \eta^{P2G}_i E^{P2G}_{i,t}, \quad 0 \le G^{P2G}_{i,t} \le \overline{G}^{P2G}_{i} \tag{7}$$

*where* $G^{B}_{i,t}, H^{B}_{i,t}$ quantify the natural gas input and thermal energy output of gas boiler i, *where* $E^{P2G}_{i,t}$ *and* $G^{P2G}_{i,t}$ characterize the electrical energy consumption and synthetic gas production in P2G device i.

The thermal output $Q^{P}_{i,t}$ and electrical generation $P^{P}_{i,t}$ of CHP unit i exhibit strong coupling characteristics,[20] with natural gas consumption represented by $G^{P}_{i,t}$. The feasible operating region for simultaneous heat and power generation is constrained within boundary curve $V_1$-$V_4$ (Figure 2), mathemati-

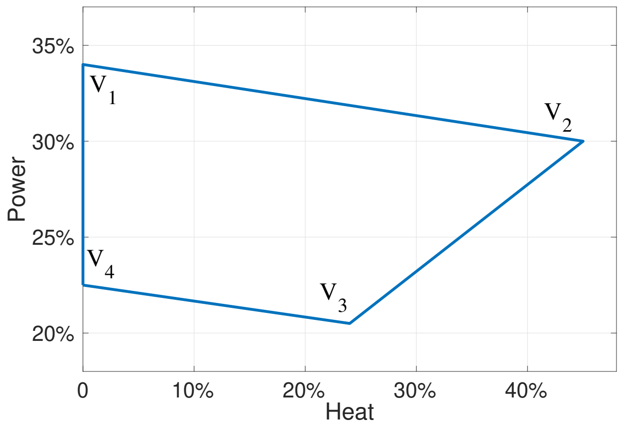


**Figure 2. Feasible operating region for heat and power generation.**

cally expressed through the following inequality constraints.

$$P^P_{i,t} - P^P_{i,V1} - \frac{P^P_{i,V1} - P^P_{i,V2}}{Q^P_{i,V1} - Q^P_{i,V2}} \left(Q^P_{i,t} - Q^P_{i,V1}\right) \le 0, \quad \forall i,t \tag{8}$$

$$P^P_{i,t} - P^P_{i,V2} - \frac{P^P_{i,V2} - P^P_{i,V3}}{Q^P_{i,V2} - Q^P_{i,V3}} \left(Q^P_{i,t} - Q^P_{i,V2}\right) \ge 0, \quad \forall i,t \tag{9}$$

$$P^P_{i,t} - P^P_{i,V3} - \frac{P^P_{i,V3} - P^P_{i,V4}}{Q^P_{i,V3} - Q^P_{i,V4}} \left(Q^P_{i,t} - Q^P_{i,V3}\right) \ge 0, \quad \forall i,t \tag{10}$$

$$0 \le Q^P_{i,t} \le Q^P_{i,V2}, \quad 0 \le P^P_{i,t} \le P^P_{i,V1}, \quad \forall i,t \tag{11}$$

The region below the boundary segment $V_1V_2$ is defined by constraint (8), while constraints (9) and (10) delimit the operational space above segments $V_2V_3$ and $V_3V_4$ , respectively. $E^P_{i,t} = P^P_{i,t}\Delta t$ and $H^P_{i,t} = Q^P_{i,t}\Delta t$ denote the electricity and heat generation from CHP unit i at time t.

## Carbon–energy market

Each BES needs to maintain equilibrium between its allocated carbon quota and real carbon emissions. According to the policy-based benchmarking method- ology, BES i is assigned a carbon emission quota $\Gamma^q_{i,t}$ . The real carbon emissions are determined by both the carbon intensity of energy consumption and the CC volume, where the carbon intensity of electricity is defined as the amount of emissions per unit of electricity generated. Thus, the real carbon emissions of BES i,[21] $\forall_i$, t, are expressed as

$$\Gamma^r_{i,t} = (1-\eta^{cc}) I^E_t E_{i,t} + I^G_t G_{i,t}, \quad \forall i,t \tag{12}$$

where $\eta^{cc}$ is the capture rate of carbon emissions. $E_{i,t}$ and $I^E_t$ are the electricity procured from the power plant and its corresponding emission intensity. $G_{i,t}$ and $I^G_t$ are the natural gas procured from the natural gas plant and the emission intensity resulting from its combustion. The carbon trading cost,[22] $\forall_i$, t, is

$$C^{ct}_{i,t} = \left\{ \begin{array}{c} -p^c(1+k\beta)\left(\Gamma^q_{i,t}-\Gamma^r_{i,t}-kl\right)-\left(k+\dfrac{(k-1)k\beta}{2}\right)p^c l, \\ \text{if } \Gamma^q_{i,t}-(k+1)l<\Gamma^r_{i,t}\le\Gamma^q_{i,t}-kl, \\ p^c(1+k\alpha)\left(\Gamma^r_{i,t}-\Gamma^q_{i,t}-kl\right)+\left(k+\dfrac{(k-1)k\alpha}{2}\right)p^c l, \\ \text{if } \Gamma^q_{i,t}+kl<\Gamma^r_{i,t}\le\Gamma^q_{i,t}+(k+1)l, \end{array} \right\} \tag{13}$$

When the allocated carbon emissions $\Gamma^q_{i,t}$ of BES i surpasses its real emissions $\Gamma^r_{i,t}$ by threshold $l$, the carbon trading price escalates by $\beta p^c$; conversely, if real emissions surpasses the carbon quota by $l$, the price will escalate by $\alpha p^c$ , where $p^c$ denotes the baseline carbon trading price. The parameters α and β correspond to the carbon price adjustment coefficients for allowance deficit and surplus scenarios, respectively. The carbon trading scheme adopts a discrete interval system with $2K$ uniformly spaced tiers, where l represents the interval width and $k \in \{0, 1, 2, \cdots, K\}$ indexes the deviation levels.

To improve energy balance and efficiency, bidirectional energy transactions are permitted among BESs, with associated transaction costs $C^B_{i,t}$ and revenues $R^S_{i,t}$ defined as.

$$C^B_{i,t} = p^e_{i,t} X^{eb}_{i,t} + p^g_{i,t} X^{gb}_{i,t}, \quad \forall i,t \tag{14}$$

$$R^S_{i,t} = s^e_{i,t} X^{es}_{i,t} + s^g_{i,t} X^{gs}_{i,t}, \quad \forall i,t \tag{15}$$

where $X^{eb}_{i,t}$ and $p^e_{i,t}$ denote the purchased electricity quantity and unit price of BES i from other BESs. $X^{gb}_{i,t}$ and $p^g_{i,t}$ denote the volume and unit price of gas procurement. $X^{es}_{i,t}$ / $s^e_{i,t}$ and $X^{gs}_{i,t}$ / $s^g_{i,t}$ denote the quantities/prices of electricity and gas sold by BES i to other BESs. Considering the nonlinearity of gas transportation, this part primarily focuses on how nodal pressure affects gas flow dynamics in gas markets. For each seller-buyer pair ij $\in \Xi$, where $\Xi$ denotes the set of BESs engaged in gas trading, the gas $X_{ij,t}$ procured by BES i from BES j is

$$X^2_{ij,t} = W^2_{ij}\left(\pi^2_{i,t} - \pi^2_{j,t}\right), \quad \forall ij,t \tag{16}$$

$$\underline{\pi} \le \pi \le \overline{\pi} \tag{17}$$

$$\underline{\rho} \le \frac{\pi_{i,t}}{\pi_{j,t}} \le \bar{\rho}, \forall ij,t \tag{18}$$

where $W_{ij}$ is the Weymouth coefficient corresponding to the pipeline connecting BES i and j, while $\pi_{i,t}$ and $\pi_{j,t}$ denote the nodal gas pressures values.

## Optimization objective

In scenarios where inter-BES energy transactions cannot meet demand, BES i will procure deficit electricity $E_{i,t}$ at tariff rate $p^e_t$, while acquiring supplemental gas supply $G_{i,t}$ at the market price $p^g_t$ from utility companies. Under renewable energy abundance scenarios, BES i may export excess generation $p^o_{i,t}$ to the power plant at the feed-in transactions price $p^{eo}_t$.

The electricity, gas and heat demand profiles of BES i are denoted by $E^L_{i,t}$, $G^L_{i,t}$ and $H^L_{i,t}$, $\forall_{i,t}$

$$E^L_{i,t} = E_{i,t} - E^o_{i,t} + X^{eb}_{i,t} - X^{es}_{i,t} + E^D_{i,t} - E^C_{i,t} + E^P_{i,t} - E^{P2G}_{i,t} + E^r_{i,t} \tag{19}$$

$$G^L_{i,t} = G_{i,t} - G^P_{i,t} - G^B_{i,t} + G^{P2G}_{i,t} + X^{gb}_{i,t} - X^{gs}_{i,t} \tag{20}$$

$$H^L_{i,t} = H^P_{i,t} + H^B_{i,t} + H^D_{i,t} - H^C_{i,t} \tag{21}$$

As derived from the preceding analysis, the total operational expenditure for BES i comprises four principal components: carbon emission trading cost, energy procurement expenses from utility providers, peer-to-peer energy transaction costs with other BESs, and BSS degradation costs.

$$Z_{i,t} = C^{ct}_{i,t} + E_{i,t}p^e_t - E^o_{i,t}p^{eo}_t + G_{i,t}p^g_t + C^B_{i,t} - R^S_{i,t} + p^{de}_t\left(E^D_{i,t} + E^C_{i,t}\right), \quad \forall i,t \tag{22}$$

where $p^{de}_t$ is the marginal degradation cost per charing/discharging cycle.

Each BES seeks to optimize its long-term economic performance by minimizing the time-averaged aggregate operational expenditure

$$\min_{Y_{i,t}} \lim_{T\to\infty} \frac{1}{T} \sum_{t=1}^{T} \mathbb{E}\{Z_{i,t}\}, \quad \forall i \tag{23}$$

s.t. (1) - (21)

where $Y_{i,t}$= $\{X^{eb}_{i,t}, X^{es}_{i,t}, X^{gs}_{i,t}, E^D_{i,t}, E^C_{i,t}, H^D_{i,t}, H^C_{i,t}, E^o_{i,t}, E_{i,t}, E^{P2G}_{i,t}, G^P_{i,t}, G^B_{i,t}, \forall i, t\}$ denote the set of decision variables in the optimization problem.

## Solution mechanism

Given the volatility of electricity market prices and intermittent renewable generation, coupled with requirements for data privacy and computational tractability, the formulated optimization cannot be addressed through conventional offline centralized methods. This necessitates a real-time distributed solution. Unlike traditional optimization methods, which demand prior knowledge of stochastic process statistics or incur prohibitive computational complexity, the enhanced Lyapunov optimization framework offers practicality by decomposing the long-term optimization problem into weighted single-interval subproblems and enabling lightweight online decision-making based on instantaneous system states while ensuring charge/discharge profit

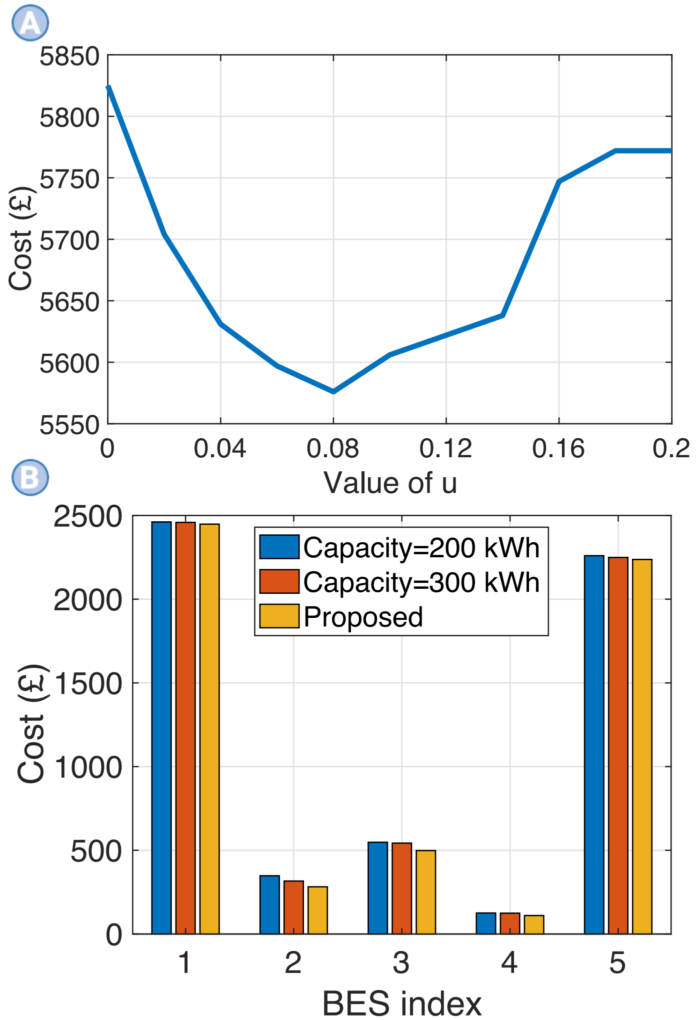


**Figure 3. (A) Variation of total cost with auxiliary variable u. (B)Costs of five BESs for three capacity levels.**

margins.

## Enhanced Lyapunov optimization

The interdependent charge/discharge dynamics of BSS (1) and TES tank (2) render direct solution of (23) infeasible. To decouple these constraints (1)-(2), the following reformulated constraints are introduced

$$\begin{aligned} \lim_{T\to\infty}\frac{1}{T}\sum_{t=1}^{T}\mathbb{E}\{E_{i,t}^{C}\} &= \lim_{T\to\infty}\frac{1}{T}\sum_{t=1}^{T}\mathbb{E}\{E_{i,t}^{D}\}, \quad \forall i \\ \lim_{T\to\infty}\frac{1}{T}\sum_{t=1}^{T}\mathbb{E}\{H_{i,t}^{C}\} &= \lim_{T\to\infty}\frac{1}{T}\sum_{t=1}^{T}\mathbb{E}\{H_{i,t}^{D}\}, \quad \forall i \end{aligned} \tag{24}$$

The optimization problem (23) is accordingly converted to its relaxed form

$$\min_{Y_{i,t}}\lim_{T\to\infty}\frac{1}{T}\sum_{t=1}^{T}\mathbb{E}\{Z_{i,t}\}, \quad \forall i \tag{25}$$

s.t. (4) - (21), (24)

Let $Z_i^o$ denote the minimal achievable cost of problem (23) across all admissible control policies and $Z_i^{or}$ denote the minimal achievable cost of problem (25). The solution of problem (25) inherently provides a performance bound for the original problem, as its constraint set is strictly contained within the original problem's feasible region. Thus, $Z_i^o \leq Z_i^{or}$ holds.

The relaxed problem admits an optimal solution achievable through a stationary randomized policy κ, stated as follows

$$E\{Z_{i,t}^{\kappa}\} = Z_i^{or}, \quad \forall i, t \tag{26}$$

subject to:

$$\begin{aligned} E_{i,t}^{C,\kappa} &= E_{i,t}^{D,\kappa} \\ H_{i,t}^{C,\kappa} &= H_{i,t}^{D,\kappa} \end{aligned} \tag{27}$$

(4) - (21)

The feasibility of this policy can be verified through Caratheodory's theorem.[17] Since the high-dimensional nature of the problem renders stationary randomized policies computationally intractable for practical implementation, Lyapunov optimization is employed to address the relaxed formulation (25).

Initially, virtual energy queues $B_{i,t} = E_{i,t}^{BSS} - \varepsilon_i$ and $M_{i,t} = H_{i,t}^{TES} - \zeta_i$ are constructed to enforce the storage capacity bound (3), where the offsets $\epsilon_i$ and $\zeta_i$ are calibrated following the methodology in ref.3. Subsequently, the Lyapunov function $L_{i,t}$ characterizing virtual energy queues, and the corresponding slot- to-slot Lyapunov drift $\Delta_{i,t}$, ∀i, t, are

$$L_{i,t} = \frac{1}{2}B_{i,t}^2 + \frac{1}{2}M_{i,t}^2 \tag{28}$$

$$\Delta_{i,t} = \mathbb{E}\left\{L_{i,t+1} - L_{i,t} \mid E_{i,t}^{BSS}, H_{i,t}^{TES}\right\} \tag{29}$$

where $\mathbb{E}\{\ \}$ is taken over the probability space generated by the system's stochas- tic processes, conditioned on $E_{i,t}^{BSS}$ and $H_{i,t}^{TES}$. Through analytical derivation, the drift is bounded as

$$\begin{aligned} \Delta_{i,t} &= \frac{1}{2}\mathbb{E}\left\{(B_{i,t+1}+B_{i,t})(B_{i,t+1}-B_{i,t})\right\} + (M_{i,t+1}+M_{i,t})(M_{i,t+1}-M_{i,t}) \\ &\leq O_i + \mathbb{E}\left\{B_{i,t}\left(E_{i,t}^{C}-E_{i,t}^{D}\right) + M_{i,t}\left(H_{i,t}^{C}-H_{i,t}^{D}\right)\right\} \end{aligned} \tag{30}$$

where $O_i = \frac{1}{2}\left[\max\left((\overline{E}_i^{C})^2, (\overline{E}_i^{D})^2\right) + \max\left((\overline{H}_i^{C})^2, (\overline{H}_i^{D})^2\right)\right]$ is a constant. The proof can be found in Ref.19.

To simultaneously minimize operational cost and energy storage fluctuations, the weight parameter $V_i$ is introduced. Through the incorporation of weighted cost terms to both sides of the above equation, it can be obtained that

$$\begin{aligned} \Delta_{i,t} + V_i\mathbb{E}\{Z_{i,t}\} \leq O_i + \mathbb{E}\{&B_{i,t}(E_{i,t}^{C}-E_{i,t}^{D}) + M_{i,t}(H_{i,t}^{C}-H_{i,t}^{D})\} \\ &+ V_i(C_{i,t}^{ct} + E_{i,t}^{e} - E_{i,t}^{o} + C_{i,t}^{B} - R_{i,t}^{S}) \\ &+ G_{i,t}p_t^{g} + p_t^{de}(E_{i,t}^{D} + E_{i,t}^{C})\}, \quad \forall i, t \end{aligned} \tag{31}$$

The problem (25) is reformulated as the minimization of the right-hand-side expression of (31)

$$\begin{aligned} \min_{Y_{i,t}} B_{i,t}&(E_{i,t}^{C}-E_{i,t}^{D}) + M_{i,t}(H_{i,t}^{C}-H_{i,t}^{D}) + V_i\left(C_{i,t}^{ct} + E_{i,t}p_t^{e}\right) \\ &- E_{i,t}^{o}p_t^{o} + C_{i,t}^{B} - R_{i,t}^{S} + G_{i,t}p_t^{g} + p_t^{de}\left(E_{i,t}^{D} + E_{i,t}^{C}\right), \quad \forall i, t \end{aligned} \tag{32}$$

s.t. (4) - (21)

Since conventional Lyapunov optimization cannot guarantee charge/discharge profitability while accounting for BSS degradation costs, auxiliary variables are incorporated into the optimization framework to enhance the effectiveness of the Lyapunov optimization approach.

As specified in equation (19), the electricity price and BSS-related components of optimization problem (32) include

$$\begin{aligned} &B_{i,t}(E_{i,t}^{C}-E_{i,t}^{D}) + V_i(E_{i,t}p_t^{e} - E_{i,t}^{o}p_t^{o} + p_t^{de}(E_{i,t}^{D}+E_{i,t}^{C})) \\ &= B_{i,t}(E_{i,t}^{C}-E_{i,t}^{D}) + V_i\left((E_{i,t}^{L} + E_{i,t}^{o} - X_{i,t}^{eb} + X_{i,t}^{es} - E_{i,t}^{D})\right) \\ &\quad + E_{i,t}^{C} - E_{i,t}^{P} + E_{i,t}^{P2G} - E_{i,t}^{r}p_t^{e} - E_{i,t}^{o}p_t^{o} + p_t^{de}(E_{i,t}^{D}+E_{i,t}^{C}) \\ &= (B_{i,t} + V_ip_t^{e} + V_ip_t^{de})E_{i,t}^{C} + (V_ip_t^{de} - V_ip_t^{e} - B_{i,t})E_{i,t}^{D} \\ &\quad + V_i\left((E_{i,t}^{L} + E_{i,t}^{o} - X_{i,t}^{eb} + X_{i,t}^{es} - E_{i,t}^{P} + E_{i,t}^{P2G} - E_{i,t}^{r})p_t^{e} - E_{i,t}^{o}p_t^{o}\right) \end{aligned} \tag{33}$$

To minimize the objective in (33), BES i initiates BSS charging when the condition $B_{i,t} + V_ip_t^{e} + V_ip_t^{de} < 0$ holds (equivalently, $p_t^{e} < -p_t^{de} - \frac{B_{i,t}}{V_i}$ ), and discharges when $V_ip_t^{de} - V_ip_t^{e} - B_{i,t} < 0$ (i.e., $p_t^{e} > p_t^{de} - \frac{B_{i,t}}{V_i}$ ).

When $p_t^{e} < -p_t^{de} - \frac{B_{i,t}}{V_i}$, the BSS charge to $E_{i,t+1}^{BSS} = E_{i,t}^{BSS} + \overline{E}_i^{C}$. If at time t + 1, the electricity price satisfies $p_{t+1}^{e} > p_{t+1}^{de} - \frac{B_{i,t+1}}{V_i} = p_{t+1}^{de} - \frac{B_{i,t+1}+E_i^{C}}{V_i}$ BSS is discharged.

To ensure net profitability after accounting for degradation, the price difference between discharging and charging $p_{t+1}^{de} - \frac{B_{i,t}+\overline{E}_i^{C}}{V_i} - \left(-p_t^{de} - \frac{B_{i,t}}{V_i}\right)$ must exceed the unit degradation cost $p_t^{de}$, where $p_t^{de}$ is assumed to be a constant. This yields the necessary condition: $p_t^{de} > \frac{\overline{E}_i^{C}}{V_i}$.

Since $p_t^{de} > \frac{\overline{E}_i^{C}}{V_i}$ may not always hold, an auxiliary term $u_i(E_{i,t}^{C} + E_{i,t}^{D})$ is intro-

**Algorithm 1 : The Optimization Mechanism**

1: Set t = 0 and initialize the energy storage $E_{i,0}^{BSS}$ and $H_{i,0}^{TES}$.
2: Determine the expected selling/purchase electricity price and gas prices based on the current stored energy and utility energy prices, and calculate the expected trading electricity and gas by solving optimization problem (35).
3: Submit expected energy transaction prices and quantities to the auctioneer.
4: Clear the market by determining the final energy prices and quantities through transmission loss minimization.
5: Compute the optimal solution by solving (35) using the cleared market results.
6: Update $E_{i,0}^{BSS}$ and $H_{i,0}^{TES}$ based on (1) and (2).

duced into (31) to ensure the net benefits of BSS operations persistently outweigh degradation costs in every time interval. Based on the preceding analysis, the inequality condition $p_{t+1}^{de} + u_i - \frac{B_{i,t} + \overline{E}_i^C}{V_i} - \left(-p_t^{de} - u_i - \frac{B_{i,t}}{V_i}\right) > p_t^{de}$ guarantees that the net revenue from charge-discharge cycles always compensates for degradation losses. Solving this inequality yields the necessary consates for degradation losses. Solving this inequality yields the necessary condition: $u_i > \frac{E_i^C}{2V_i} - \frac{p_t^{de}}{2}$. An analogous condition for discharging operations requires: $u_i > \frac{E_i^D}{2V_i} - \frac{p_t^{de}}{2}$. These inequalities collectively determine the lower bound constraint for the auxiliary parameter $u_i$

$$u_i > \frac{\max\left(\overline{E}_i^C, \overline{E}_i^D\right)}{2V_i} - \frac{p_t^{de}}{2} \tag{34}$$

After integrating the auxiliary variable $u_i$, problem (32) is transformed as

$$\begin{aligned} \min_{Y_{i,t}} B_{i,t}\left(E_{i,t}^C - E_{i,t}^D\right) + M_{i,t}\left(H_{i,t}^C - H_{i,t}^D\right) + V_i\left(C_{i,t}^{ct} + E_{i,t}p_t^e - E_{i,t}^o p_t^o + C_{i,t}^B - R_{i,t}^S\right) \\ + G_{i,t}p_t^g + \left(p_t^{de} + u_i\right)\left(E_{i,t}^D + E_{i,t}^C\right), \quad \forall i,t \end{aligned} \tag{35}$$

s.t. (4) - (21)

### Pricing and clearing mechanism

To obtain the optimal solution for the aforementioned problem, two key challenges must be addressed: First, the quadratic constraint (16) for gas trans- mission must be addressed. Then, the BES pricing transaction problem requires resolution. For the first challenge, a boundary-tightening algorithm based on quadratic constraint relaxation is introduced to ensure effective constraint handling.[23] Regarding the second challenge, the auction method with a pricing mechanism is employed to implement trading among BESs.

To safeguard the economic benefits of participants and accurately capture the authentic trading demands, a pricing mechanism based on the current state of their energy storage systems and energy prices of utility companies is pre- sented to determine the expected electricity/gas selling and purchase prices of BESs as follows: $\tilde{s}_{i,t}^b = \max\left[\frac{-B_{i,t}}{V_i}, p_t^{eg}\right], \tilde{s}_{i,t}^b = \max\left[\frac{-\eta_i^{bg}A_{i,t}}{V_i}, p_i^{Bg}\right], \tilde{p}_{i,t}^e = \min\left[\frac{\max\left(-B_{i,t},0\right)}{V_i}, p_t^e\right], \tilde{p}_{i,t}^g = \min\left[\frac{\eta_i^{b_i}\max\left(-A_{i,t},0\right)}{V_i}, p_t^g\right], \forall i,t.$

Upon receiving all expected energy price submissions, the auctioneer sorts the selling electricity prices in increasing order and the purchasing electricity prices in decreasing order.[24]

$$\begin{aligned} \hat{s}_{1,t}^e \le \hat{s}_{2,t}^e \le \cdots \le \hat{s}_{j,t}^e \le r_e \le \hat{s}_{j+1,t}^e \le \cdots \le \hat{s}_{n,t}^e \\ \hat{p}_{1,t}^e \ge \hat{p}_{2,t}^e \ge \cdots \ge \hat{p}_{i,t}^e \ge r_e \ge \hat{p}_{i+1,t}^e \ge \cdots \ge \hat{p}_{m,t}^e \end{aligned} \tag{36}$$

When i = j, the sellers 1, 2,..., j and the buyers 1, 2,..., i can trade at electricity price $r_e$. When i > j, the sellers 1, 2,...j and the buyers 1, 2,..., j can trade electricity, where the purchase price is $\hat{p}_{j+1,t}^e$ and the selling price is re. When i < j, the sellers 1, 2,..., i and the buyers 1, 2,..., i can trade electricity, where the purchase price is re and the selling price is $\hat{s}_{i+1,t}^e$. The gas prices among BESs are determined through an analogous mechanism. Following the determination of energy trading prices and participants, buyers and sellers are optimally matched through energy transmission loss minimization.

Subsequently, the solution to the optimization problem is derived based on the finalized trading quantities and clearing prices. The proposed mechanism is shown in Algorithm 1.

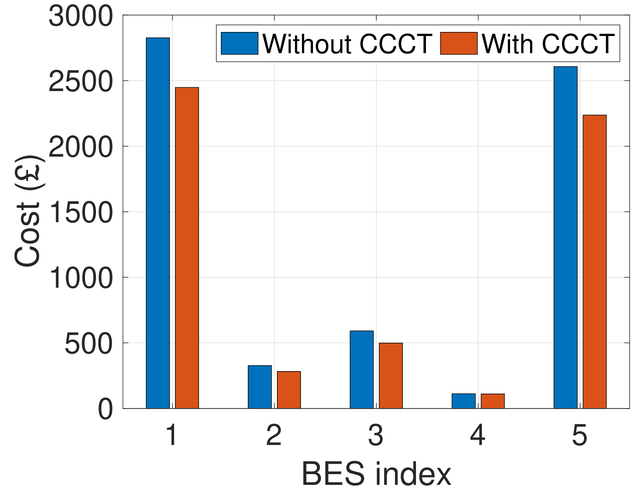


**Figure 4. Comparison of five BESs without and with CCCT.**

### Performance analysis

The analysis of BSS and TES capacity constraints is as follows.

**Lemma 1.** The tradeoff term $V_i$ and offset terms $\boldsymbol{\epsilon}_i$, $\zeta_i$are chosen as:

$$\overline{V}_i = \min\left\{\frac{\overline{E}_i^{BSS} - \overline{E}_i^C - \overline{E}_i^D}{\overline{p}^e}, \frac{\eta_i^{BG}\left(\overline{H}_i^{TES} - \overline{H}_i^C - \overline{H}_i^D\right)}{\overline{p}^g}\right\}$$

$$0 \leqslant Vi \leqslant Vi \tag{37}$$

$$\varepsilon_i = V_i\bar{p}^{\mathbf{e}} + \bar{E}_i^{\mathbf{D}}$$

$$\zeta_i = \frac{V_i\bar{p}^S}{\eta_i^{BG}} + \overline{H}_i^D$$

, the BSS and TES capacity constraints of BES i can be ensured to meet.

Lemma 1 guarantees that the proposed methodology maintains the capacity constraints of both BSS and TES, thereby ensuring the solutions obtained for problem (25) are feasible for the original problem (23). The performance characteristics of this approach are quantified in the following theorem.

**Theorem 1.** The proposed method yields a system cost bounded as follows:

$$L_{i,t} = \frac{1}{2}B_{i,t}^2 + \frac{1}{2}M_{i,t}^2 \tag{38}$$

The proof of Lemma 1 and Theorem 1 can refer to Ref.17.

The performance bound analyzed in Theorem 1 reveals that the proposed scheme's effectiveness improves with larger energy storage capacity or higher values of $V$, enabling arbitrary closeness to the theoretical optimum. However, Lemma 1 imposes an upper bound on $V$, as surpassing this limit might violate the fundamental energy storage capacity restrictions.

## RESULTS

### Simulation setup

This paper investigates carbon-energy trading among multiple buildings.

The load profiles of five buildings are sourced from a university campus located in central London, UK, as shown in Figure S1A. Energy prices are obtained from,[25] shown in Figure S1B, while PV generation data is derived from Renewables.ninja.[26] Based on the building energy loads, their maximum renewable energy outputs are 600 kW, 480kW, 540kW, 180kW, and 600kW, respectively. Key parameters are summarized in Table S1.

To verify the proposed method, a mixed-integer programming based two-stage method without renewable energy (MITS) similar to,[27] a conventional Lyapunov optimization without auxiliary variable ui (LOWA) similar to,[28] and a bi-level bargaining-based method (BLBM) similar to[29] are adopted. Given

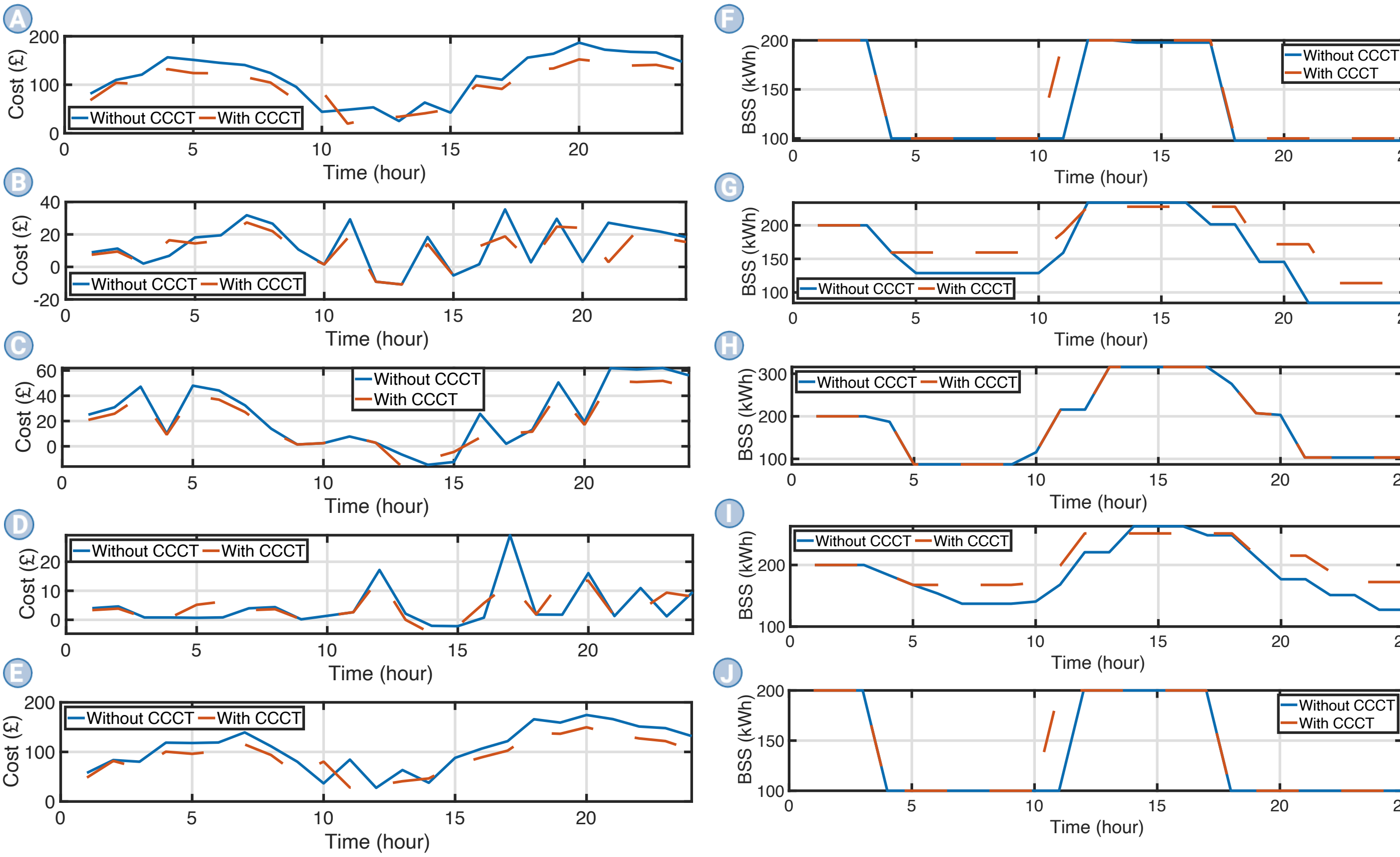


**Figure 5. Cost across five BESs with and without CCCT.**

identical energy storage capacity and charge/discharge energy limits for each BES, Lemma 1 indicates that all $V_i$ parameters share the same value, hereafter uniformly denoted as *V*. The same to $u_i$.

### Enhanced Lyapunov optimization

This section examines the impact of auxiliary variable u within the enhanced Lyapunov optimization framework on system operational costs to identify its optimal value and demonstrate the efficacy of the proposed approach. When u = 0, the proposed algorithm is the conventional Lyapunov optimization method. The total daily costs demonstrate significant parametric dependence as u varies across the range of 0 to 0.2 £/kWh, as illustrated in Figure 3A.

For parameter values below the threshold $u \le \frac{\max\left(\bar{E}^C, \bar{E}^D\right)}{2V} - \frac{p_t^{da}}{2}$ the achievable benefit from charge/discharge operations is insufficient to compensate for BSS degradation expenses. Progressive elevation of u within this range gradually narrows the gap between operational gains and degradation losses, producing a corresponding reduction in daily expenditures. Thus, when $u \le \frac{\max\left(\bar{E}^C, \bar{E}^D\right)}{2V} - \frac{p_t^{da}}{2}$, as u increases, the total weekly costs decrease.

When the auxiliary variable exceeds this threshold, i.e. $u > \frac{\max\left(\bar{E}^C, \bar{E}^D\right)}{2V} - \frac{p_t^{da}}{2}$ further increases in u impose more stringent criteria for BSS arbitrage, necessitating substantially wider electricity price differentials between charging and discharging periods. As a result, the BSS exclusively performs charge/discharge cy- cles when encountering higher profits, potentially leading to the oversight of cer- tain profit opportunities. Thus, the total daily cost initially decreases followed by subsequent growth. At the specified parameter value of u = 0.08, the proposed enhanced Lyapunov optimization approach guarantees that charge/discharge revenues consistently surpass degradation expenses, while simultaneously maximizing the utilization of both the BSS capacity and available electricity price arbitrage opportunities.

Figure 3B presents the cost comparison of five BESs with BSSs and TES

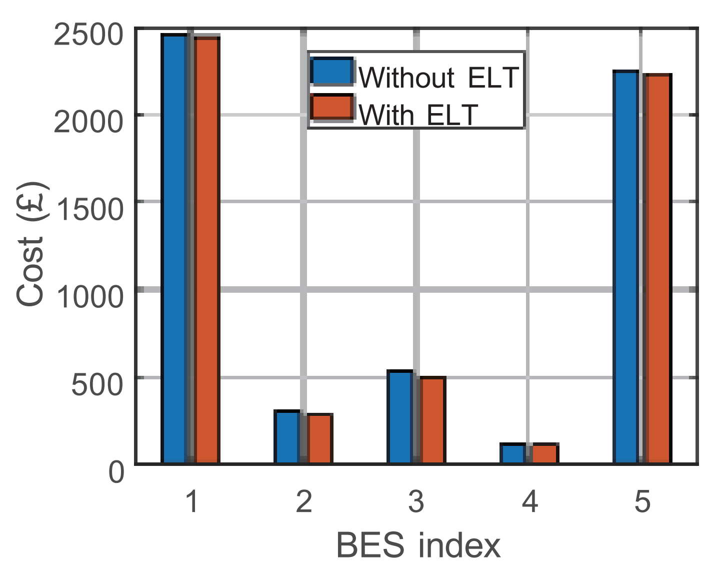


**Figure 6. Cost of five BESs without and with ELT.**

tanks at varying capacity configurations. The observed inverse relationship between energy storage capacity and operational cost validates the effectiveness of the enhanced Lyapunov optimization and provides empirical confirmation of Lemma 1 and Theorem 1.

### Coordinated carbon capture and trading

To satisfy the emission mandates of BESs, the mechanism employs coordinated CC alongside ladder incentive-penalty carbon trading (CCCT). Figure 4, 5A-E and Table S2 demonstrate that the proposed CCCT mechanism achieves cost reductions for BESs. The BESs with CCCT flexibly adjust carbon trading and capture volumes based on cost minimization. The total

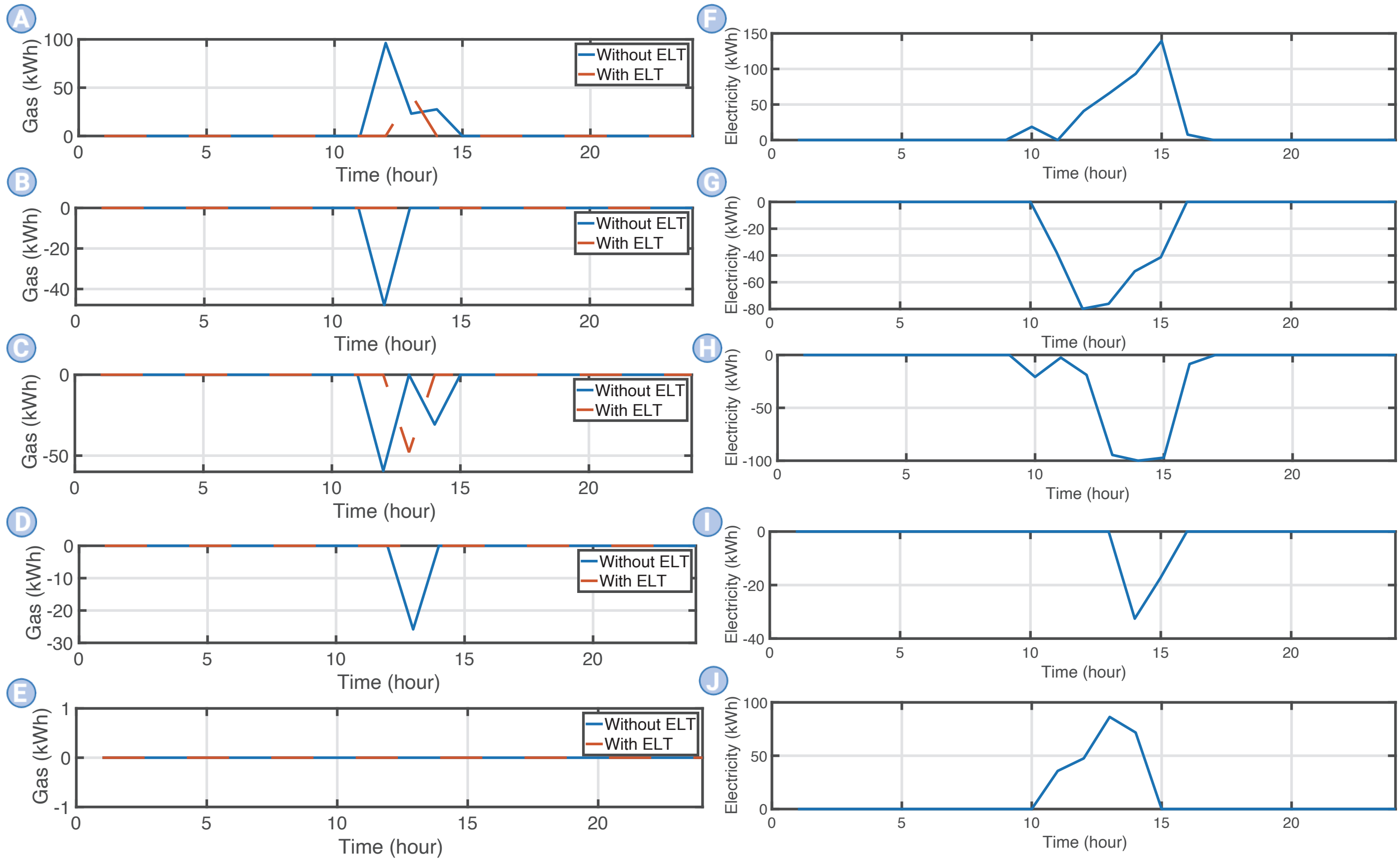


**Figure 7. Gas traded across five BESs.**

operational costs for BESs comprise energy procurement expenses from utility companies and other BESs, CCCT costs. The energy and carbon markets operate at distinct tem- poral resolutions, with trading intervals of one hour and one day, respectively. Comparative daily cost profiles under CCCT-enabled and CCCT-disabled scenarios are presented in Table S2.

Given that the efficiency of power plant with maximum CC power (PPMP) is 85%, BESs lacking CCCT will purchase electricity from the PPMP to cir- cumvent regulatory sanctions. The embedded CC costs are internalized into electricity prices, resulting in PPMP tariffs exceeding conventional grid rates. When the carbon trading cost exceeds the CC cost, the BES with CCCT will preferentially deploy CC to mitigate the excess emissions. The residual emis- sions are then offset through carbon credit transactions, thereby maintaining equilibrium between emissions output and allocated quotas.

With the implementation of CCCT, BESs 1 and 5 experience significant cost reductions while BES 4 sees only a minor decrease. This is because BESs 1 and 5 is produce considerably higher carbon emissions compared to BES 4, which emits little. BESs 1 and 5 capture much carbon emissions by purchas- ing low- carbon electricity from PPMP, leading to more costs. In contrast, the carbon emissions of BES 4 are close to its carbon quota, resulting in minimal change. In Figure 5F-J the absence of CCCT in BESs leads to decreased BSS charging, consequently lowering the need to purchase expensive electricity from PPMP.

## Energy trading

BESs can participate in energy trading to either sell excess generation or procure additional energy from other BESs. In energy trading, positive values indicate energy purchases, while negative values represent energy sales. Figure 6 demonstrates that the implementation of electricity trading (ELT) reduces operational costs across all five BESs. Figuer 7A-E demonstrates that the BESs without ELT compensate for energy deficits through increased gas trading activity, where the gas traded is generated by P2G. Since BESs 2-4 generates more elec- tricity than their consumption by its PV system in daylight, it can sell excess energy to BESs 1 and 5 instead of selling to the power plant at a lower price, as shown in Figure 7F-J Thus, the cost of BESs 2 and 3 is reduced more. The PV generation of BES 4 slightly exceeds its electricity consumption during the day- time, resulting in only a modest cost reduction. BESs 1 and 5 without ELT can purchase more gas from other BESs to make up the deficient electricity which cannot be purchased from other BESs, where some generated gas are used for heating generation. Thus, although BESs 1 and 5 cannot purchase the low-price electricity from other BESs, it still does not incur high costs.

Figure 8A shows that electricity and gas trading (EGT) achieves cost reductions across all five BESs, with slight reductions for BESs 1, 4 and 5, and significant reductions for BESs 2-3. BESs 2-3 with EGT can sell surplus much energy to BESs 1 and 5, avoiding low-price sales to the power plant, resulting in significant cost reductions. BES 4 with EGT sell little energy to BESs 1 and 5, leading to slight cost reductions. Although BESs 1 and 5 without EGT cannot access energy trading among BESs, they can obtain heat and elec- tricity by CHP rather than buying electricity from the power plant at premium rates. This results in modest cost reductions for BESs 1 and 5. It is worth noting that when the installed capacity of renewable energy is larger or when there is greater energy trading among BESs, more cost reductions can be achieved.

Given that energy trading, CC and carbon trading are not yet widely im- plemented in BESs, Figure 8B compares the costs of the proposed approach with a baseline method that excludes CCCT and EGT, demonstrating the superior cost-efficiency of our solution.

## Method comparison

Figure 8C & D illustrates the cost performance of five BESs under four strategies: MITS, LOWA, BLBM and the proposed method. The costs under MITS are comparable to those of the proposed method during the period from 0:00-5:00. Nevertheless, renewable energy scarcity forces BESs under MITS to purchase more energy during the day, leading to higher costs and carbon emissions.

The economic gains from charging/discharging operations in LOWA do not consistently outweigh the associated BSS degradation costs, resulting in

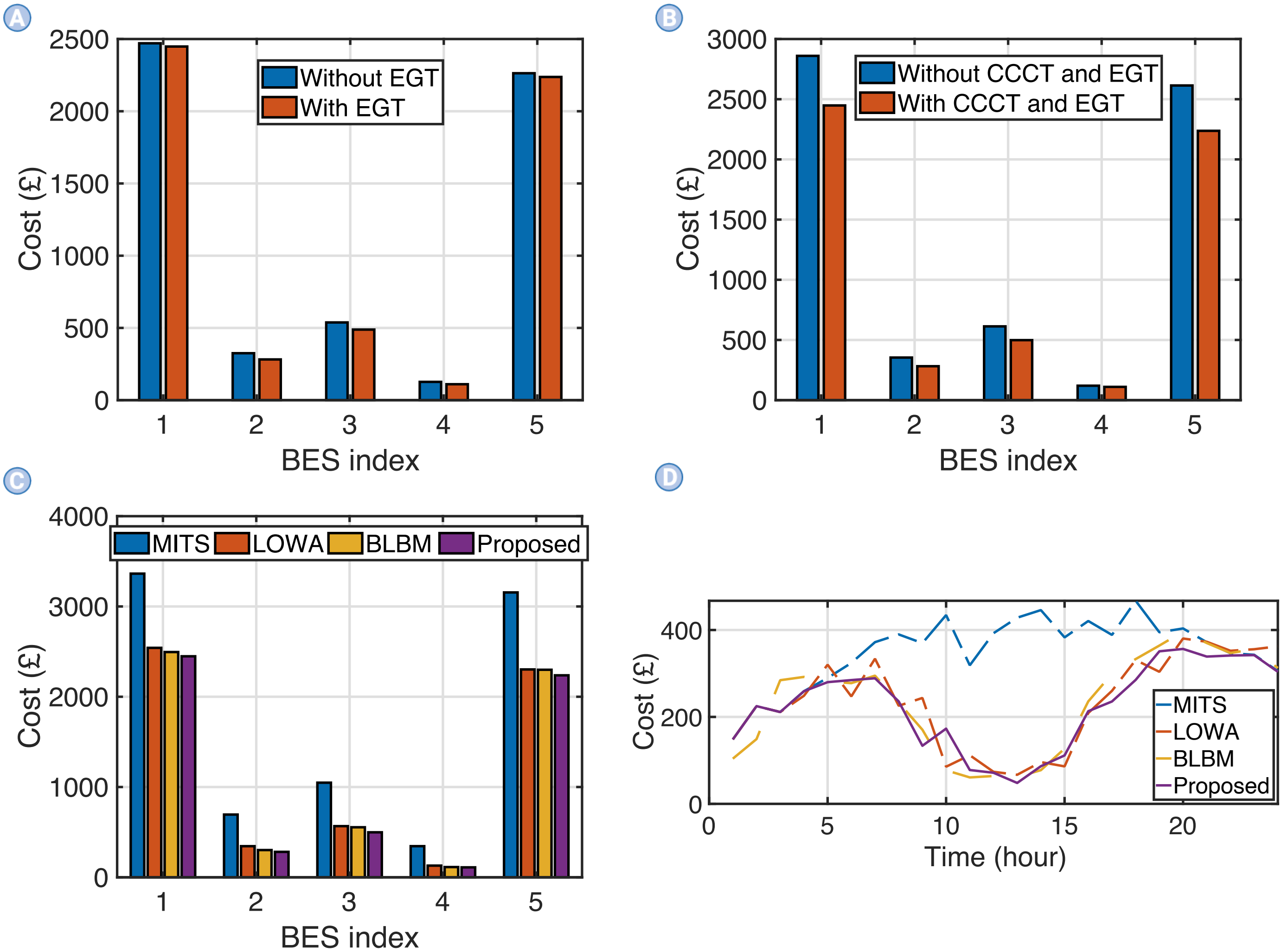


**Figure 8. Comparison of five BESs without and with EGT.**

suboptimal economic performance. Under BLBM, BESs fail to fully exploit the potential of energy storage systems, leaving valuable flexibility untapped and leading to increased costs. In contrast, the proposed algorithm efectively leverages energy storage, optimizes real-time energy scheduling, minimizes time-average operational costs, and ensure a more economical and low-carbon operation.

## CONCLUSION

An integrated energy management framework for multi-buildings is constructed, where the coordinated operation of energy storage, CC and P2G enhances local renewable energy utilization while enabling carbon emissions recycling through pipeline injection of synthesized natural gas. To alleviate the imbalance of supply/demand and carbon emissions/quota, an electricity and gas trading mechanism, along with tiered incentive-penalty carbon trading and capture approach, is presented in this paper. The joint trading and scheduling method integrates an enhanced Lyapunov optimization with a market clearing mechanism, ensuring charging/discharging benefits without relying on prior

knowledge of stochastic processes. Simulation shows that each BES reduces costs and emissions while improving energy efficiency and ensuring resource balance by the proposed mechanism.

In future work, a significantly larger number of BESs may participate in carbon-energy trading, reflecting more realistic, large-scale deployment scenar- ios. Moreover, building energy efficiency and carbon emissions can be further improved through the effective management of flexible energy demands. Thus, extending the joint trading and scheduling framework to include a broader range of buildings - as explored in -[30] is of considerable importance. Additionally, optimizing the scheduling of energy devices, as discussed in,[31] is crucial for enhancing overall energy efficiency and unlocking greater demand response potential.

Furthermore, ethical considerations in carbon, gas, and electricity trading are also important, focusing on issues of fairness, justice, and the effectiveness of market-based mechanisms in reducing emissions. Future research should exam- ine the potential for inequities and injustices associated with these mechanisms under specific circumstance such as social housing and care home with vulner- able population.

## REFERENCES

1. Global Status Report. (2025). Global Status Report for Buildings and Construction 2024/2025. https://www.developmentaid.org/api/frontend/cms/file/2025/03/Global-Status-Report-2024-2025.pdf.
2. Zheng Z., Tang R., Luo X., et al. (2024). A distributed coordination strategy for heterogeneous building flexible thermal loads in responding to smart grids. *IEEE Trans. Smart Grid.* **15**:1620–1633. DOI:10.1109/TSG.2023.3306044
3. Zhu D., Yang B., Li L., et al. (2025). Industrial energy management and production decision making via Lyapunov-guided learning. *IEEE Trans. Smart Grid* **16**:2184–2196. DOI:10.1109/TSG.2025.3549723
4. Tang R., Li H. and Wang S. (2019). A game theory-based decentralized control strategy for power demand management of building cluster using thermal mass and energy storage. *Appl. Energy* **242**:809–820. DOI:10.1016/j.apenergy.2019.03.152
5. Antoniadou-Plytaria K., Steen D., Tuan L.A., et al. (2021). Market-based energy management model of a building microgrid considering battery degradation. *IEEE Trans. Smart Grid* **12**:1794–1804. DOI:10.1109/TSG.2020.3037120
6. Nikkhah S., Allahham A., Royapoor M., et al. (2022). Optimising building-to-building and building-for-grid services under uncertainty: A robust rolling horizon approach. *IEEE Trans. Smart Grid* **13**:1453–1467. DOI:10.1109/TSG.2021.3135570

7. He B., Zhang N., Fang C., et al. (2024). Flexible building energy management with neural ODEs-based model predictive control. *IEEE Trans. Smart Grid* **15**:4690–4704. DOI:10.1109/TSG.2024.3401227
8. Saberi H., Zhang C. and Dong Z.Y. (2024). A multi-agent deep constrained Q-learning method for smart building energy management under uncertainties. *IEEE Trans. Smart Grid* **15**:4649–4661. DOI:10.1109/TSG.2024.3386896
9. Wu Z., Chen Z., Ren Y., et al. (2025). Data-driven analysis of the interaction between storage ownership and market behavior. *IEEE Trans. Ind. Appl.* **61**:1735–1747. DOI:10.1109/TIA.2024.3462304
10. Jin X., Wang X., Jia H., et al. (2025). Peer-to-peer multi-energy trading among heterogeneous building prosumers via asynchronous distributed algorithm. *IEEE Trans. Smart Grid* **16**:1590–1603. DOI:10.1109/TSG.2024.3483280
11. Yu L., Yue D., Tan Y., et al. (2024). Online distributed coordination operation for grid-interactive efficient residential buildings. *IEEE Trans. Smart Grid* **15**:3639–3652. DOI:10.1109/TSG.2023.3339761
12. Yang Y., Hu G. and Spanos C.J. (2021). Optimal sharing and fair cost allocation of community energy storage. *IEEE Trans. Smart Grid* **12**:4185–4194. DOI:10.1109/TSG.2021.3083882
13. X. Chen, A. Sun, W. Shi and N. Li, "Carbon-Aware Optimal Power Flow," IEEE Transactions on Power Systems, doi: 10.1109/TPWRS.2024.3514516.
14. Yang Y., Shi J., Wang D., et al. (2024). Net-zero scheduling of multi-energy building energy systems: A learning-based robust optimization approach with statistical guarantees. *IEEE Trans. Sustain. Energy* **15**:2675–2689. DOI:10.1109/TSTE.2024.3437210
15. Yan Z., Li C., Yao Y., et al. (2023). Bi-level carbon trading model on demand side for integrated electricity-gas system. *IEEE Trans. Smart Grid* **14**:2681–2696. DOI:10.1109/TSG.2022.3229278
16. Yu L., Xu Z., Guan X., et al. (2023). Joint optimization and learning approach for smart operation of hydrogen-based building energy systems. *IEEE Trans. Smart Grid* **14**:199–216. DOI:10.1109/TSG.2022.3197657
17. Lakshminarayana S., Quek T.Q.S. and Poor H.V. (2014). Cooperation and storage tradeoffs in power grids with renewable energy resources. *IEEE J. Sel. Areas Commun.* **32**:1386–1397. DOI:10.1109/JSAC.2014.2332093
18. Yu L., Xie D., Huang C., et al. (2019). Energy optimization of HVAC systems in commercial buildings considering indoor air quality management. *IEEE Trans. Smart Grid* **10**:5103–5113. DOI:10.1109/TSG.2018.2875727
19. Chen S., Zhang S., He S. and Yang H. (2025). Two-timescale online optimization of behind-the-meter battery storage for stacked revenue by providing multi-services. *IEEE Trans. Smart Grid* **16**:2222–2233. DOI:10.1109/TSG.2025.3538014
20. Chen Y., Wei W., Liu F., et al. (2019). Energy trading and market equilibrium in integrated heat-power distribution systems. *IEEE Trans. Smart Grid* **10**:4080–4094. DOI:10.1109/TSG.2018.2849227
21. Wang Y., Qiu J. and Tao Y. (2022). Optimal power scheduling using data-driven carbon emission flow modelling for carbon intensity control. *IEEE Trans. Power Syst.* **37**:2894–2905. DOI:10.1109/TPWRS.2021.3126701
22. Zhang C. and Kuang Y. (2024). Low-carbon economy optimization of integrated energy system considering electric vehicles charging mode and multi-energy coupling. *IEEE Trans. Power Syst.* **39**:3649–3660. DOI:10.1109/TPWRS.2023.3280067
23. Chen Y. and Zhao C. (2023). Improved approximation of dispatchable region in radial distribution networks via dual SOCP. *IEEE Trans. Power Syst.* **38**:5585–5597. DOI:10.1109/TPWRS.2022.3226894
24. Wang Y., Saad W., Han Z., et al. (2014). A game-theoretic approach to energy trading in the smart grid. *IEEE Trans. Smart Grid* **5**:1439–1450. DOI:10.1109/TSG.2013.2284664
25. Elexonportal.co.uk, https://bmrs.elexon.co.uk/market–index–prices.
26. Renewables.ninja, https://www.renewables.ninja.
27. Chen Y., Wei W., Liu F., et al. (2017). A multi-lateral trading model for coupled gas-heat-power energy networks. *Appl. Energy* **200**:180–191. DOI:10.1016/j.apenergy.2017.05.060
28. Yan D. and Chen Y. (2023). A distributed online algorithm for promoting energy sharing between EV charging stations. *IEEE Trans. Smart Grid* **14**:1158–1172. DOI:10.1109/TSG.2022.3203522
29. Zou Y., Xu Y., Feng X. et al. (2023). Peer-to-peer transactive energy trading of a reconfigurable multi-energy network. *IEEE Trans. Smart Grid* **14**:2236–2249. DOI:10.1109/TSG.2022.3223378
30. Cui S., Wang Y.W. and Xiao J.W. (2019). Peer-to-peer energy sharing among smart energy buildings by distributed transaction. *IEEE Trans. Smart Grid* **10**:6491–6501. DOI:10.1109/TSG.2019.2906059
31. Tang R. and Wang S. (2019). Model predictive control for thermal energy storage and thermal comfort optimization of building demand response in smart grids. *Appl. Energy* **242**:873–882. DOI:10.1016/j.apenergy.2019.03.038

## FUNDING AND ACKNOWLEDGMENTS

This work was supported by the UCL Global Engagement Funds.

## DECLARATION OF INTERESTS

The authors declare no competing interests.

## DATA AND CODE AVAILABILITY

Data are available from the corresponding author upon reasonable request.

## SUPPLEMENTAL INFORMATION

Supplementary materials are available at: https://doi.org/10.59717/ipj.energy-use.2025.100003